Integrating Spheres for Mid- and Near-infrared Reflection Spectroscopy

Leonard M. Hanssen and Keith A. Snail

Reproduced from:

Handbook of Vibrational Spectroscopy

John M. Chalmers and Peter R. Griffiths (Editors)

Integrating Spheres for Mid- and Near-infrared Reflection Spectroscopy

Leonard M. Hanssen[1] and Keith A. Snail[2]

[1] *National Institute of Standards and Technology, Gaithersburg, MD, USA*
[2] *Naval Research Laboratory, Washington, DC, USA*

1 INTRODUCTION

Integrating sphere instrumentation has historically been the primary analysis tool for accurate quantitative characterization of reflectance and absorptance of samples and materials that exhibit a high degree of scattering. The four most widely used types of instruments for performing reflectance measurements of diffusing surfaces are biconical mirror systems, gonio-reflectometers, 2π conic mirror reflectometers, and integrating spheres. Spectrophotometer accessories of biconical design (e.g. "praying mantis" type devices) are the most commonly used for semiquantitatively characterizing the diffuse reflectance of powdered samples. However, because of the restricted angular range of measurement, a fraction of the reflected light that is dependent on the specific directional scattering properties of each sample will be lost. This limits the degree of accuracy for these devices. For quantitative measurements of hemispherical diffuse reflectance, methods based on the 90+ years of accumulated knowledge on integrating spheres are preferred. Two comprehensive reviews of absolute methods for integrating sphere-based reflectance measurements were published in the 1970s by Budde[1] and the International Commission on Illumination (CIE).[2] Since that time, integrating spheres for the mid-infrared have become commonplace, and major advances have occurred in the areas of computational optics modeling of integrating spheres, coupling detectors to spheres with nonimaging concentrators, and the development of new nearly Lambertian reflectors.

A single article must necessarily be focused on specific aspects of integrating sphere reflectance spectroscopy. In this article we will describe the integrating sphere instrumentation that is used in diffuse reflection spectroscopy: how sphere systems function, what the various designs and methods for reflectance and transmittance measurement are, both absolute and relative, what the sources of measurement error are, and why sphere systems are used in preference to other techniques. We begin by defining the specialized terms associated with diffuse reflectance measurement in Section 2, followed by a short historical review of the important developments in the use of integrating spheres for reflectance in Section 3. The most important characteristic parameter of an integrating sphere, its throughput (efficiency), is discussed in Section 4. This provides an introduction to a detailed description and comparison of both absolute and relative methods that are used in sphere systems in Section 5. Sources of error and measurement uncertainty are addressed in Section 6. A sampling of current commercial sphere reflectometer systems is described in Section 7, followed by a summary in Section 8.

2 TERMINOLOGY

A clear set of definitions distinguishing the various possible geometrical configurations for reflectance and transmittance are a prerequisite to understanding the various methods and sphere designs that are currently in use for measurement. The terminology used throughout this article will be that of the CIE,[3] with a few minor modifications. Many of the commonly used terms are defined in this volume's

glossary. More specialized terms relating to integrating spheres and reflectance, not included in the handbook glossary, are defined below. All the terms can have a wavelength dependence that is usually implied, but can also be made explicit through addition of the modifier "spectral" to each term.

- *reflectance* ρ*:* the ratio of flux reflected from a surface to that incident on the same surface (this is the general case, without reference to a particular incident beam or collection geometry).
- *reflectance factor R:* the ratio of flux reflected from a surface to that reflected from a perfect reflecting diffuser under the same incident beam geometry.
- *directional-hemispherical reflectance* $\rho_{h,d}$*:* reflectance, where the incident flux is confined (in a narrow range) to a single direction (θ,ϕ) and the reflected flux is collected over the complete hemisphere above the surface, where θ and ϕ are polar and azimuthal angles, respectively, relative to the sample surface.
- *hemispherical-directional reflectance factor* $R_{h,d}$*:* reflectance factor, where the incident flux is uniformly distributed over the hemisphere above the surface, and the measured reflected flux is collected (in a narrow range) in a single direction (θ,ϕ).
- *hemispherical-hemispherical (bi-hemispherical) reflectance* $\rho_{h,h}$*:* the ratio of reflected to incident flux on a surface, where both the incident and reflected fluxes are taken over the complete hemisphere.
- *bidirectional reflectance factor* $R_{d,d}$*:* reflectance factor, where both the incident and reflected fluxes are confined and collected, respectively (in a narrow range) to specific directions.
- *biconical reflectance factor* $R_{c,c}$*:* reflectance factor, where both the incident and reflected fluxes are confined (in a narrow range) to cones with specific central and width half-angles.
- *bidirectional reflectance distribution function (BRDF)* $f(\gamma;\theta,\phi)$*:* the ratio of reflected radiance from, to incident irradiance on, a surface, where γ represents the input angle geometry, as, for example 8 degrees off normal, and θ,ϕ the exit angles of the reflected light. This quantity gives a complete description of the manner in which a sample reflects light.

  All of the terms above have analogous counterparts for *transmittance*.
- *integrating sphere throughput* (or simply, *throughput*), $\tau = \Phi_d/\Phi_0$*:* the efficiency of the integrating sphere system, where Φ_d is the flux incident on the detector, and Φ_0 the input flux.
- *measurement ratio*, V_s/V_r, of sample, V_s to reference, V_r signals or single beam spectra.

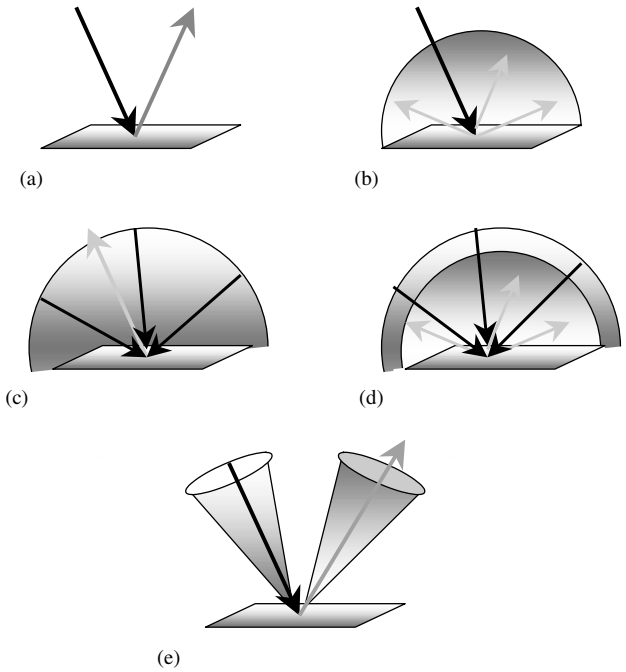

Figure 1. Reflectance measurement geometries. (a) Bidirectional: single direction input and single direction detected; (b) directional-hemispherical: single direction input and detection over all angles; (c) hemispherical-directional: uniform input over all angles and single direction detection; (d) bi-hemispherical: uniform input over all angles and detection over all angles; and (e) biconical: uniform input over a range of angles within a cone of defined half angle centered on a single input direction and detection over a second (usually similar) cone.

- *exchange factor* of the *ith* sphere port f_i, which, for an integrating sphere, $= A_i/A_{sp}$, the ratio of port area A_i to sphere area A_{sp}.

As an aid to the reader to understand the meaning of the more important reflectance terms, graphical versions are shown in Figure 1.

3 HISTORICAL REVIEW

In 1892, Sumpner[4] presented a simple expression for the throughput of a spherical enclosure coated with a diffuse reflector. Although Sumpner's work was motivated by the need to predict the enhanced brightness of a room's walls due to multiple reflections, it became the seminal work for the integrating sphere field. Within a decade, Ulbricht[5] had developed a photometer for measuring the brightness of lamps that was based on this principle. In 1916, Rosa and Taylor[6] developed the first technique for measuring the absolute reflectance of a diffuse surface with an integrating sphere. Four years later, Taylor,[7] Benford[8] and Sharp and Little[9] all published new sphere-based absolute reflectance techniques. These early advances in the integrating sphere field were later reviewed and added to

by Karrer,[10] Benford[11] and Taylor.[12] In 1928, the diffuse reflectance and colorimetry fields leaped forward with the development of the first recording spectrophotometer by Hardy[13] at MIT. Hardy's instrument was based on a dispersive double-prism design and an integrating sphere, and was subsequently commercialized by General Electric.[14]

Prior to 1960, most near-infrared sphere measurements utilized an MgO sphere coating,[15] with $BaSO_4$ becoming more popular after that time. For many decades the only option for performing spectral diffuse reflectance measurements in the mid-infrared was a conic mirror reflectometer,[16] due to the absence of suitable mid-infrared integrating sphere coatings. In 1966, Morris fabricated a glass sphere with a roughened, aluminized surface for use beyond 3.0 μm. About 10 years later, Egan and Hilgeman tested a sphere coated with sulfur flowers for use in the 0.15–12 μm region. A major advance in instrumentation occurred in 1976 with the introduction of the Willey 318 infrared (IR) diffuse spectrophotometer.[17] Willey's innovative instrument, shown in Figure 2, utilized a Michelson interferometer, an integrating sphere with a diffuse textured gold surface, and a double-beam geometry. In the 1980s Labsphere commercialized diffuse gold integrating spheres. IR sphere accessories are now available for most commercial Fourier transform infrared (FT-IR) spectrophotometers. The National Physical Laboratory (NPL) in the UK provides a flame-sprayed aluminum diffuse reflectance standard artefact.[18] The National Institute of Standards and Technology (NIST) in the USA is also developing an IR diffuse reflectance standard based on roughened gold.

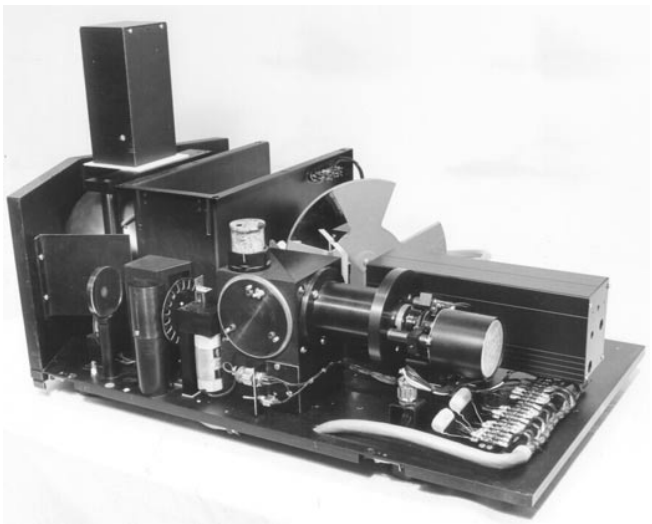

Figure 2. Willey's IR integrating sphere spectrophotometer with internal components exposed. The integrating sphere can be seen in the back left of the structure with a rectangular housed detector mounted on its top. In the front area is the interferometer block, with the moving mirror drive at the front right, and calibrating laser just behind it. Also visible is the section of a large reflecting chopper wheel to switch between sample and reference beams. (Reproduced by permission of R.R. Willey.)

Another significant development in the integrating sphere field was the introduction[19] of nonimaging concentrators[20] for coupling detectors and sources to spheres. Most absolute sphere designs depend on either a restricted field of view (FOV) detector or a hemispherical FOV detector. The combination of nonimaging concentrators and baffles can be used[21] to eliminate measurement errors associated with unequal scattering of radiation from the sample and reference into the sphere wall region viewed by the detector. Nonimaging concentrators also have the advantage of returning rejected light into the sphere, which results in significant enhancements in throughput[22] compared with baffling or collimating a detector's FOV.

4 THEORY OF SPHERE THROUGHPUT

Integrating sphere accessories are the instruments of choice for accurate quantitative spectroscopy of scattering materials. Their design allows measurement of directional-hemispherical reflectance, hemispherical-directional reflectance factor and/or hemispherical-hemispherical reflectance. Two features of integrating spheres are critical to their ability to accurately measure reflected fluxes. The first is that the interior surface has (ideally) a Lambertian coating of high reflectance. This means that the radiance of the coating is constant in all directions. The second important feature is the spherical shape of the interior. For a Lambertian scattering surface, light incident on it results in a constant irradiance over any spherical shell that contains the surface. Hence light incident anywhere on an integrating sphere is immediately uniformly distributed over its entire surface. A detector located on the spherical surface or viewing a part of it will always receive flux that is directly proportional to the light incident on the sphere, independent of location. Even if the sphere surface is not perfectly Lambertian, the high reflectance of the surface leads to a large number of reflections around the sphere prior to absorption of the incident light. This cavity effect further contributes to the uniform flux distribution over the sphere interior. Thus, when light is incident on a sample with arbitrary BRDF, the sphere can be used to accurately collect all the reflected flux.

For the measurement of sample reflectance, an approach to analyzing the behavior of an integrating sphere is to examine its throughput, or efficiency. There are several approaches to calculating the sphere throughput. These include (a) using conservation of energy, or "energy balance" within the sphere;[23] (b) solving an integral equation of the sphere irradiance;[24–26] (c) summing up irradiance or

absorbed flux components by following successive reflections within the sphere;[27,28] and (d) solving a matrix equation with matrices of size $n \times n$ determined by n, the number of distinct regions of the sphere.[29,30] Clare[31] performed a comparative analysis of all four methods and established a consistency of results. The simple form for the throughput for a simplified sphere (all ports curved to match sphere) can be expressed as:

$$\tau = f_{\mathrm{d}} \frac{\rho_{\mathrm{w}}}{1 - \bar{\rho}_{\mathrm{w}}} \tag{1}$$

where f_{d} is the exchange factor between the detector and sphere wall, which is equal to (for a sphere), $A_{\mathrm{d}}/A_{\mathrm{sp}}$, the ratio of the detector area to the sphere area, ρ_{w} is the sphere wall hemispherical reflectance, and $\bar{\rho}_{\mathrm{w}}$ is the average sphere wall reflectance, defined as

$$\bar{\rho}_{\mathrm{w}} = \rho_{\mathrm{w}} \left(1 - \sum_i f_i \right) + \sum_i f_i \rho_i \tag{2}$$

where the summations are made over all ports or regions of the sphere with hemispherical reflectance different from the wall's, f_i is the exchange factor between the ith port and sphere wall, which equals A_i/A_{sp}, the ratio of the ith port area to the sphere area, and ρ_i is the ith port hemispherical reflectance.

The throughput equations are derived based on the important assumption that the sphere wall and all ports including the sample are Lambertian diffusers. This allows each one to be represented by a single reflectance value, i.e.

$$\rho_{\mathrm{d,h},j} = \rho_{\mathrm{h,h},j} = \rho_j \tag{3}$$

The throughput, denoted by equation (1), represents the relative flux completely measured by an ideal detector that has no angular variation in response. However, real detectors have angular response variation, both due to the inherent physics of the detecting element, as well as to FOV restrictions such as windows, apertures or baffles. These effects need to be included in integrating sphere calculations to obtain more accurate results. Hanssen[28] examined the FOV effects and derived the throughput equation

$$\tau = f_{\mathrm{d}} \left[\eta_{\mathrm{s0}} + \frac{f_{\mathrm{v}} \bar{\rho}_{\mathrm{v}}}{1 - \bar{\rho}_{\mathrm{w}}} \right] \tag{4}$$

where f_{v} is the exchange factor between the detector FOV and the sphere wall, which equals $A_{\mathrm{v}}/A_{\mathrm{sp}}$, the ratio of the FOV area to the sphere area, $\bar{\rho}_{\mathrm{v}}$ is the average reflectance of the FOV, and η_{s0} is the fraction of the incident beam falling within the FOV. Simplified forms can be obtained from equation (4) for specific situations such as a hemispherical detector FOV ($\eta_{\mathrm{s0}} = 1$, $\bar{\rho}_{\mathrm{v}} = \bar{\rho}_{\mathrm{w}}$, $f_{\mathrm{v}} = 1$, then $\tau = f_{\mathrm{d}}/(1 - \bar{\rho}_{\mathrm{w}})$).

5 REFLECTANCE TECHNIQUES

The implementation of the integrating sphere for reflectance measurements of nonspecular or scattering samples has over time taken a number of forms. These have been methods, each employing a unique sphere design, for both relative and absolute characterization of reflectance. The sphere designs apply equally well to all spectral regions including the near- and mid-infrared.

5.1 Absolute reflectance methods

Although relatively few in number when compared with the more ubiquitous relative reflectance instruments, integrating spheres designed for absolute reflectance measurement play a very important role. This is because only absolute method spheres (or other hemispherical measurement devices) can be used to calibrate the standards that are required for relative reflectance instruments. Seven traditional absolute methods and a relatively new hybrid method developed by one of the authors will be discussed briefly in this section.

Using a method for measuring absolute reflectance based on an integrating sphere with minimal measurement uncertainty is not a simple exercise. For most "absolute sphere" methods, integrating sphere theory, including evaluation of sphere throughput as described in Section 4, is used to arrive at the final absolute results. A number of implicit assumptions such as the ideal (Lambertian) nature of the sphere coating, and omission of the secondary effects of baffles exist in the basic versions of these methods. Some of these methods over time have been refined and developed into new variations that deal with these assumptions.

The first four traditional absolute methods were, quite remarkably, all developed nearly simultaneously and published in 1920. These are described in papers by Benford,[8] Sharpe and Little,[9] and Taylor[7] (two methods). The next two methods were realized using spheres with samples centrally located inside the sphere. These have been described in publications by Korte and Schmidt,[32] and Edwards *et al*.[33] The last traditional absolute method was developed in 1966 by Van den Akker *et al*.[34] Common to all these methods is the reliance on analytical sphere theory and/or an effective limitation of applicability to only nearly ideal sphere coatings and samples, i.e. nearly Lambertian as well as with very high reflectance. This allows the use of a single value for $\rho_{\mathrm{d,h}}$, $R_{\mathrm{h,d}}$, and $\rho_{\mathrm{h,h}}$, as in equation (3), and results in minimal differences between the sample and reference or sphere wall reflectance. In fact two of the methods (Benford and Van den Akker) require the sample material to be used as the sphere coating itself. Recently, Hanssen[35,36] has implemented a method that avoids reliance

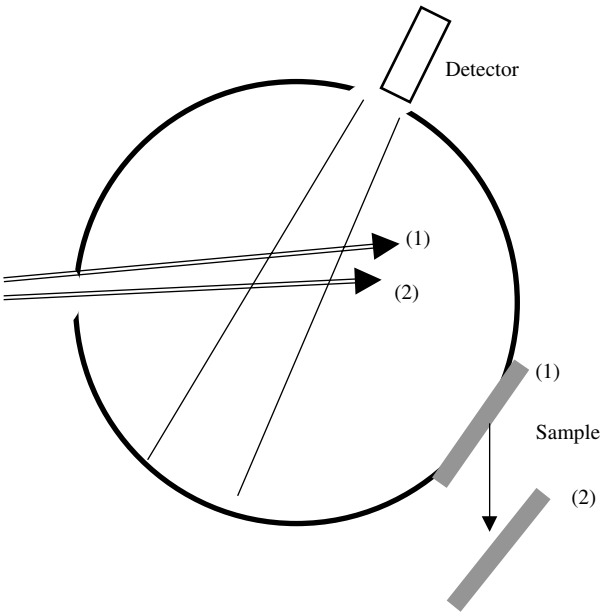

Figure 3. Taylor's $\rho_{h,h}$ absolute method and Benford's absolute method. Sample and reference measurements are indicated by (1) and (2), respectively. The input beam is incident on the sphere wall in the same location for both measurements, while a sample is mounted on the sphere wall in (1) and removed for (2). Benford's method is identical to Taylor's except that a curved sample section is used that matches the rest of the sphere, resulting in simpler equations.

on sphere theory, a sample's ideal characteristics and associated assumptions.

In his paper, Taylor described five methods for determining reflectance. Two of these are absolute in that they do not entail comparison with a previously measured standard. The procedure for one of the methods Taylor described in his 1920 paper is shown in Figure 3. This method determines the bi-hemispherical reflectance of a material that is first used to coat the integrating sphere as well as a flat sample. The sphere has entrance, sample and detector ports, and is coated with the material to be characterized. Measurement #1 is made with a flat sample (of the same material as the sphere coating) covering the sample port, the input light incident on the sphere wall in one region, and the detector viewing the sphere wall in another region. A second measurement, #2, is made with identical input and viewing geometry, except that the sample is removed, leaving an open sample port. The measurement ratio can be used to determine the absolute bi-hemispherical reflectance of the sample. Additional relative measurements can be made on samples of other materials not used to coat the entire sphere. Further refinements of this Taylor method, including more accurate formulations, were made by Preston,[37] and Middleton and Sanders.[38] As the relative sample port size becomes very small,[39] this method approaches that of Benford, for which the bi-hemispherical reflectance can be written as:

$$\rho_{h,h} = \left(1 - \sum_i f_i\right) + \frac{f_{cap}}{V_s/V_r - 1} \tag{5}$$

where $f_{cap} = A_{cap}/A_{sp}$ is the exchange factor between the sample port or "cap" and the sphere wall, and the summation is over all other ports (assumed to have "0" reflectance). In Benford's method, the sample is a section of the sphere itself, so that when it is in place the spherical shape is maintained. This allows the simple formulation of equation (5), whereas the use of flat samples requires the use of a more complicated equation. Refinements to Benford's method were made by Miller and Sant[40] and Hanssen,[41] to include consideration of the detector FOV.

The second absolute method described in Taylor's 1920 paper is shown schematically in Figure 4. The sample measurement (#1) has incident light on the sample and the detector viewing a separate sphere region (the detector FOV) that is shaded from direct illumination from the sample by means of an intervening baffle. The reference measurement (#2) has the same detector viewing geometry, but the input light is incident on a region that is not baffled from the detector FOV. The directional-hemispherical reflectance, as a function of the measurement ratio, is given by:

$$\rho_{d,h} = \frac{V_s/V_r}{1 - \sum_i f_i} \tag{6}$$

This equation assumes the implicit shading effect of the baffle, but otherwise includes no further baffle effects. Taylor

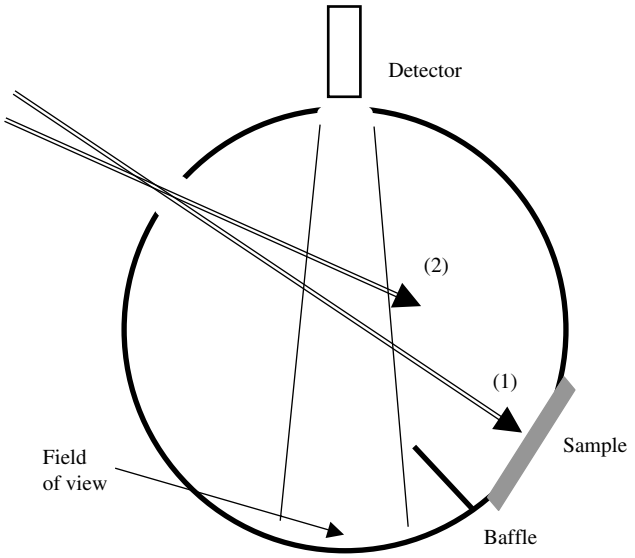

Figure 4. Taylor's $\rho_{d,h}$ absolute method. (1) The input beam is directed onto the sample which is baffled from directly scattering into the detector FOV. (2) Then it is directed onto the sphere wall in a location that is not baffled from the detector FOV.

did not include any corrections to V_s/V_r in his description. These were developed later by others, including Reule.[42] After noting deficiencies in the application of equation (6) to their Taylor method sphere, Sheffer *et al*.[43,44] developed additional corrections to account for secondary shadowing effects of the baffle.

The method developed by Sharp and Little[9] and later refined by Budde and Dodd[45] is an inversion of Taylor's directional-hemispherical method that produces an absolute hemispherical-directional reflectance value,

$$R_{h,d} = \frac{V_s/V_r}{1 - \sum_i f_i} \tag{7}$$

This can be seen from Figure 5, which shows the measurement geometries involved. The sphere has the same arrangement as in Figure 4, except that the input source and detector are switched. In the sample measurement (#1), the detector views the sample, while the input beam is incident on a region of the sphere that is shaded by the baffle from direct illumination by the sample. For the reference measurement (#2), the detector views another sphere region that is not baffled from the directly illuminated region. Due to symmetry with Taylor's method, the same equation should apply, except for the reflectance quantity. The Sharpe–Little method is currently used at the National Research Council (NRC) in Canada for reflectance in the ultraviolet–visible–near-infrared (UV–vis–NIR) spectral region.

The Van den Akker (or "double sphere") method[34] was developed as a means to calibrate a nearly ideal standard

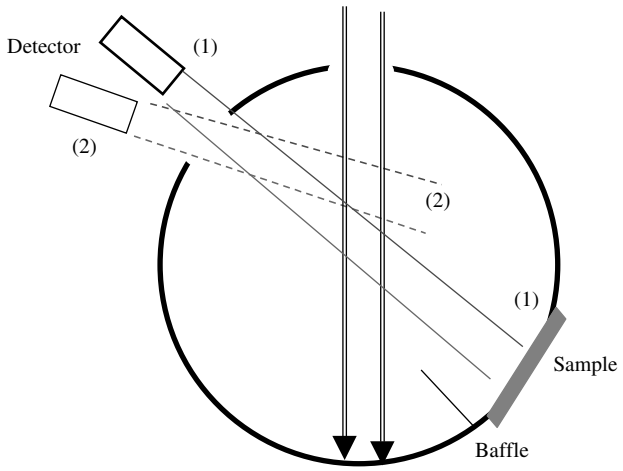

Figure 5. Sharp–Little's $R_{h,d}$ absolute method, the inverse (exchange source and detector) of Taylor's $\rho_{d,h}$ absolute method. (1) The input beam illuminates a region on the sphere that is baffled from the sample, while the detector views the sample. (2) Then the detector views another region on the sphere wall that is not baffled from the input beam.

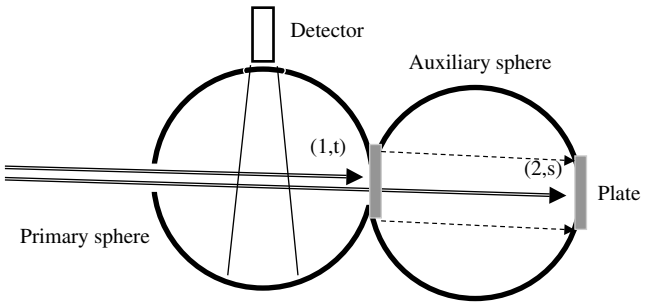

Figure 6. Van den Akker's double sphere $\rho_{h,h}$ absolute method. (1) An initial measurement is made with a sample plate mounted on the primary sphere with the input beam incident on it. (2) The plate is then mounted on a secondary sphere (coated with the same material as the sample plate), which is itself mounted onto the primary sphere sample port. The input beam is incident on the sample plate in the secondary sphere at the same angle as on the primary sphere.

material and is used to determine the bi-hemispherical reflectance, $\rho_{h,h}$. Two integrating spheres are used as shown in Figure 6. A comparison is made between a flat sample plate in one measurement and a secondary sphere coated with the same material mounted on the sphere's port for a second measurement. The arrangement shown in Figure 6 is used at NIST in the USA for the UV–vis–NIR spectral range. From the measurements,

$$\rho_{h,h} = \frac{1 - f(V_t/V_s)[1/(1-\alpha)]}{1 - f} \tag{8}$$

where f is the ratio of sample port to secondary sphere areas, and α is an additional term described by Venable *et al*.[46] in a more refined evaluation of the method. Supplementary measurements of the relative angular dependence of $\rho_{d,h}$ using a center-mount sphere, similar to one described below, are used in combination with $\rho_{h,h}$ from equation (8) to finally obtain absolute values for $\rho_{d,h}$.

Two methods are based on "center mount" sphere designs in which the sample is located at the sphere's center. Tingwaldt[47] constructed a sphere with a fixed sample centered in the sphere and the source mounted internal to the sphere. An external detector alternately viewed the sample through a port, and then the sphere wall as a reference. The ratio obtained is $R_{h,d}$. To the extent that uniform illumination could be received at the sample, this ratio provides a nominally absolute result. Toporets[48] modified the design by replacing the internal source with input from an external monochromator. Korte and Schmidt[32] significantly improved upon Tingwaldt's design by introducing six sources baffled from directly illuminating the sample. They were able to demonstrate uniform illuminance in their sphere to within 0.1%. Further variations were introduced by Erb,[49,50] including location of a single source back to

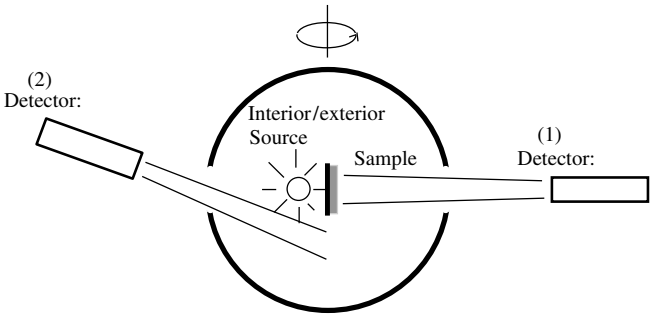

Figure 7. Korte–Schmidt's center mount $R_{h,d}$ absolute method. The source is located at the sphere center, mounted back to back with the sample (with a reflective shield in between). (1) The detector views the sample directly. (2) Then the sphere is rotated so that the detector views the sphere wall in the hemisphere above the sample, via a second port.

back with the sample (separated by a baffle). This is the system currently in use at the Physikalische Technische Bundesanstalt (PTB) in Germany. Erb's design is shown schematically in Figure 7.

$$R_{h,d} = \frac{V_s/\overline{V}_r}{1 - 4f_e} \tag{9}$$

where f_e is the entrance port exchange factor, and the factor of 4 represents the increase due to the centrally located sample. The reference measurement, which is denoted by the bar, is averaged over several locations. The denominator in equation (9) is the factor k_1 in equation (11) of Erb.[50]

Edwards *et al.*[33] interchanged the detector and source in Toporet's design arrangement to obtain a method for determination of $\rho_{d,h}$. The input beam is switched between incidence on the sample to incidence on the sphere wall behind the sample. His design shown in Figure 8, has become known as the "Edwards Sphere", and is manufactured commercially. The reflectance obtained for a Lambertian sample, as in the case of the Korte method, is

$$\rho_{d,h} = \frac{V_s/V_r}{1 - 4f_e} \tag{10}$$

All of the absolute methods described above and their later refined versions make use of nearly ideal sphere coatings, such as poly(tetrafluoroethylene) (PTFE) and $BaSO_4$ in the visible (i.e. nearly Lambertian and very high (>0.98) in reflectance) to obtain absolute reflectance values. In addition, the best materials for which the absolute reflectance can be determined most accurately (and which become standard artefacts) are those same sphere coating materials. These conditions allow integrating sphere theory to be used with high accuracy. Even with nearly ideal coatings and standard samples, corrections to the equations described above are required at each of the National

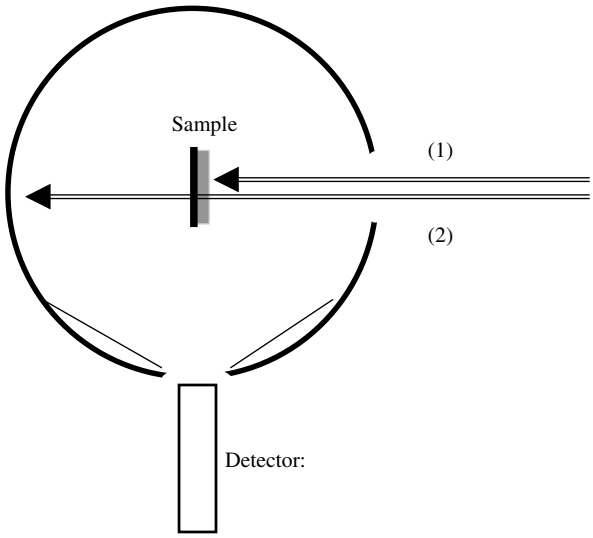

Figure 8. Edwards' center mount $\rho_{d,h}$ absolute method. (1) The input beam is incident on the sample. (2) Then the sphere is rotated about the entrance port so that the beam bypasses the sample and is directly incident on the sphere wall in the hemisphere behind the sample.

Measurement Institutes (NMIs) (National Standards Laboratories) to obtain the highest accuracy. For samples in general with a potentially wide range of parameter values (including reflectance value and BRDF), and for the IR spectral regions beyond 2.5 μm where available sphere coating materials are less ideal, these absolute methods do not work as well. Where some of these absolute methods have been implemented for the IR, significant (greater than several percent) errors and discrepancies can be obtained.[51]

These factors motivated the development of an alternative absolute method that could be applied to the measurement of arbitrary samples and spheres with nonideal coatings by Hanssen and Kaplan[36] for use in the IR beyond 2.5 μm. The method is not limited to any particular arrangement of sample, reference, entrance and detector ports, or the existence or location of baffles. It can be employed by or adapted to most sphere designs. The method has been applied to an existing sample-wall-mount sphere design with symmetrically positioned sample and reference ports shown in Figure 9.[36] In the sample reflectance measurement the input beam enters the sphere through the entrance port. For a standard *relative* measurement, the reference measurement beam would be incident on a standard located in the reference port. To obtain a result that is as close as possible to an *absolute* measurement, the reference beam enters the sphere through the reference port and strikes the sphere wall.[36] For the specular sample case due to the high degree of symmetry of this arrangement, the ratio of these measurements gives a "raw" absolute reflectance

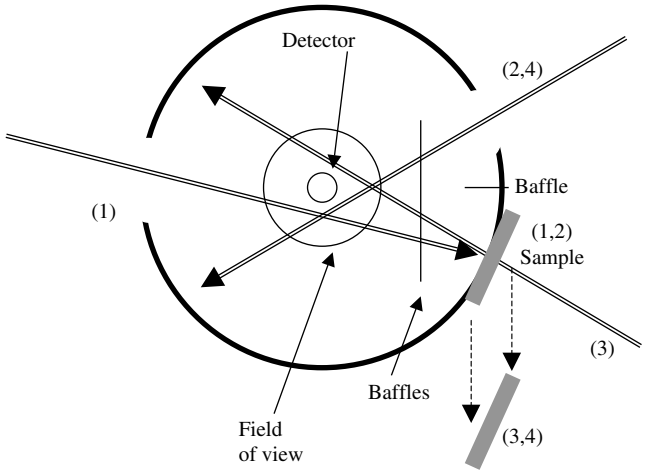

Figure 9. $\rho_{d,h}$ absolute method sphere geometry of Hanssen.[36] The view is from above (in contrast to the previous diagrams). (1) The input beam is incident on the sample, while the detector views a FOV region that is baffled from the sample. (2) Then the sphere is rotated about two axes so that the input beam enters the sphere through a second port (that otherwise functions as a reference sample port – see Figure 10), and is incident on the sphere wall location not baffled from the FOV. After the sample is removed, a second pair of measurements are made. (4) The reference measurement is repeated, and (3) a measurement is made with the beam entering the sphere through the sample port after a pair of rotations. Additional measurements, including sphere throughput variation mapping and sample BRDF, are combined with the direct sphere measurements to obtain $\rho_{d,h}$.

value that can be within a few tenths percent of the correct value.

For a nonspecular sample, if the integrating sphere were ideal (i.e. had spatially uniform [constant] throughput over the entire sphere), the sample to reference ratio would be a direct measurement of the absolute directional-hemispherical reflectance of the sample, for any sample BRDF. The error (or uncertainty) in this simple measurement of the reflectance is determined by the extent to which the real sphere deviates from the ideal. Other absolute methods apply corrections to the simple ratio that are calculated using integrating sphere theory. In contrast, the method described by Hanssen[36] employs directly measured values to determine the appropriate corrections. In it the refined directional-hemispherical reflectance value is obtained by combining four measured quantities: (a) the ratio of sample (V_s) to reference (V_r) measurements with the sphere system ((#1) and (#2) in Figure 9), V_s/V_r; (b) the ratio of sample-removed (V_{0s}) to reference measurements (V_{0r}) ((#3) and (#4) in Figure 9), V_{0s}/V_{0r}; (c) the relative sphere throughput, as a function of polar (θ) and azimuthal (ϕ) angles (relative to the sample normal) obtained through measurement, $\tau_s(\theta,\phi)/\tau_{s0}$, where τ_{s0} is the throughput for the direction corresponding to the sample-removed measurement; and (d) the relative BRDF of the sample for the incidence (γ) angle of the sphere measurement, $f(\gamma;\theta,\phi)/f_0$, where f_0 is an arbitrary constant.

These four quantities are used to determine the absolute directional-hemispherical reflectance as given by

$$\rho_{\gamma,h} = \frac{V_s}{V_r}\frac{V_{0r}}{V_{0s}} \times \left[\frac{\int_0^{2\pi}\int_0^{\frac{\pi}{2}} f(\gamma;\theta,\phi)/f_0 \cdot \sin(2\theta)\cdot d\theta\cdot d\phi}{\int_0^{2\pi}\int_0^{\frac{\pi}{2}} f(\gamma;\theta,\phi)/f_0 \cdot \tau_s(\theta,\phi)/\tau_{s0}\cdot \sin(2\theta)\cdot d\theta\cdot d\phi}\right] \quad (11)$$

Details of the derivation and additional discussion are presented in the Appendix. Simplified forms are obtained for specific cases: if the sample is Lambertian, the bracket term reduces to a denominator of τ_s/τ_{s0} averaged over the hemisphere; if the throughput is constant except for empty ports, the bracket reduces to a denominator term of $(1-\Sigma f_i)$ as in equations (6) and (7); and if the sample is specular the bracket term equals 1, and the directional reflectance

$$\rho_{\gamma,\gamma} = \frac{V_s}{V_r}\frac{V_{0r}}{V_{0s}} \quad (12)$$

The simplified direct specular case has been used for obtaining high-accuracy measurements for windows, mirrors and similar samples using the same sphere described herein.[52] Other sphere arrangements can be used with this method. The high degree of symmetry in the design shown in Figure 9 is desirable to minimize error and uncertainties, but is not a requirement for use of the method. The reference measurements (V_r, V_{0r}) can, in principle, be made in several ways (i.e. input beam on the sphere wall or a reference sample), provided the sample-removed measurement (V_{0s}) is aligned as shown in Figure 9.

5.2 Relative reflectance methods

For routine optical characterization of the vast variety of materials that are used in industrial and other research laboratories, as well as in processing and in the field, relative reflectance method spheres are commonly used. Sphere design considerations for these applications can be quite different than those for the measurement of absolute reflectance of nearly ideal standards. Relative methods start with known reference standards, often both specular and diffuse. Comparisons are made relative to these standards. The primary goal of relative methods should be to treat the reflected light from the standard and the samples under test in the same way. Another way to state this is to have

identical throughput for the sample and standard. For an ideal sphere devoid of baffles and ports and having an ideal Lambertian coating, this goal can be achieved easily. This is because for an ideal sphere, the throughput is uniform throughout the sphere and the detector receives the same proportion of input flux (and an ideal detector will produce a constant signal) independent of the scattering distribution of the sample or reference. However, the ideal situation as described above is not easily realized. Neither spheres nor detectors are ideal, hence the detected signal observed from a sample measurement will vary depending on the sample's scattering distribution and the sphere's throughput uniformity. A more detailed discussion of these effects can be found in Section 6.

Relative reflectance integrating spheres can be divided into two types: substitution mode and comparison mode spheres. A substitution mode sphere is one with a single mount or port that is used for both (alternately) sample and reference. A comparison mode sphere is one that uses two ports (or equivalent, such as a sample port and a sphere wall location) to accommodate both sample and reference simultaneously, and also a mechanism for moving either the sphere or input beam (or detector viewing area for h/d reflectance factor systems) to switch between sample and reference measurements. A substitution mode sphere is the simplest design. It can be very compact and requires no moving parts as well as no relative motion between the input/output beams and the integrating sphere. Its major drawback is that the sphere throughput changes between sample and reference measurements as can be seen from equation (4). The error can be partially corrected for depending on the detailed knowledge of the sphere parameters such as the wall reflectance and relative port sizes. For the comparison mode both the sample and reference remain in the sphere for both sample and reference measurements and no correction is necessary. A typical comparison mode design, using ports in the sphere wall for sample and reference locations, for relative reflectance, is shown in Figure 10. The location of the ports and baffles is designed to maximize the degree of symmetry between the sample and reference measurements. As described in Section 6.2, baffles play an important role in the design shown. They are used to block direct interchange of light between the sample and reference, and the detector and its FOV.

A second class of sphere designs for reflectance are the "center mount" sphere designs, for which two absolute methods were described in Section 5.1. This type of sphere could be either substitution or comparison mode. Again a substitution mode "center mount" design would involve no moving parts, except as required to access the sample. A comparison mode sphere might have the sample and reference mounted back to back on a rotatable mount to switch between sample and reference measurements.

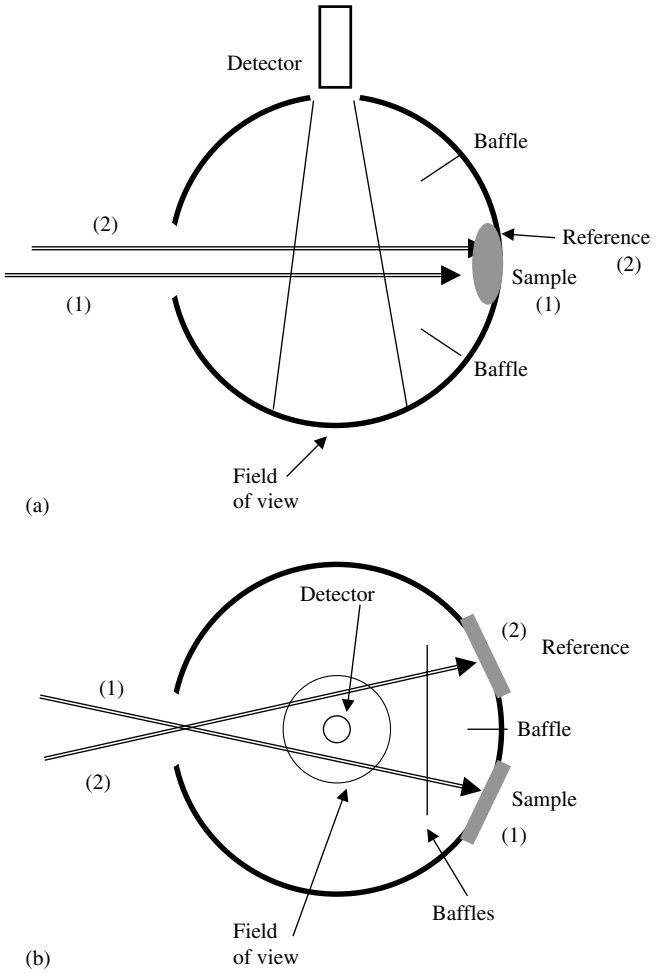

Figure 10. Typical relative reflectance measurement geometry. Side (a) and top (b) views show the locations of entrance, detector, FOV, sample and reference ports designed for maximum symmetry between sample (1) and reference (2) measurements. In the collapsed side view of (a), the reference is hidden behind the sample. Baffles are used to prevent any direct reflection between any pair of the sample, reference, detector or detector FOV (except only for the pair of the latter two). Baffle effects are discussed in Section 6.2.

6 DEALING WITH ERROR SOURCES: SPHERE DESIGN CONSIDERATIONS

An ideal diffuse reflectometer can be defined as a reflectometer with a throughput that is independent of the angle of reflected radiation, as measured at the sample. Effects due to ports, baffles, the sample's BRDF, the detector FOV, the sphere coating's BRDF and the curvature of samples can all introduce systematic measurement errors. The purpose of this section is to review the sphere design features

and principles that will minimize these sources of error. We assume that the sphere considered has its sample and reference simultaneously mounted on the wall and is operated in the comparison mode in a d/h geometry. The error sources and effects described here also apply to "substitution" mode spheres (with a single port for both sample and reference). However, as discussed in Section 5.2, such spheres have increased levels of measurement error and will not be addressed specifically here. Detailed descriptions of the substitution error can be found in Hardy and Pineo[53] and others.[24,25]

6.1 Detector field of view and sphere symmetry

After the reflection of the input beam from the sample and reference, the reflected light will be distributed on the sphere wall according to the sample and reference BRDFs. For accurate measurement results, an equal fraction of the reflected sample and reference radiation must illuminate the sphere wall region viewed by the detector.[21] If the radiation exchange factors from the sample and reference to the sphere wall viewed by the detector are not equal, a systematic measurement error will be introduced. After the first reflection from the sphere wall, the residual radiation that was reflected from the sample and reference will have equal radiation exchange factors to the sphere wall viewed by the detector if the sphere wall coating is Lambertian. There are only three detector FOV–sphere geometries[21,26] that guarantee (irrespective of BRDF) that equal fractions of sample- and reference-reflected radiation is scattered into the region of the sphere wall viewed by the detector. The three geometries have detectors with a hemispherical FOV, a FOV that includes exactly half of the sphere wall, and a FOV that is restricted to a narrow angular region. These three ideal sphere geometries can be implemented with nonimaging concentrators[54] and are shown in Figure 11(c), (b) and (a), respectively. Analogous inverse geometries for measurement of $R_{h,d}$ are also feasible.[21]

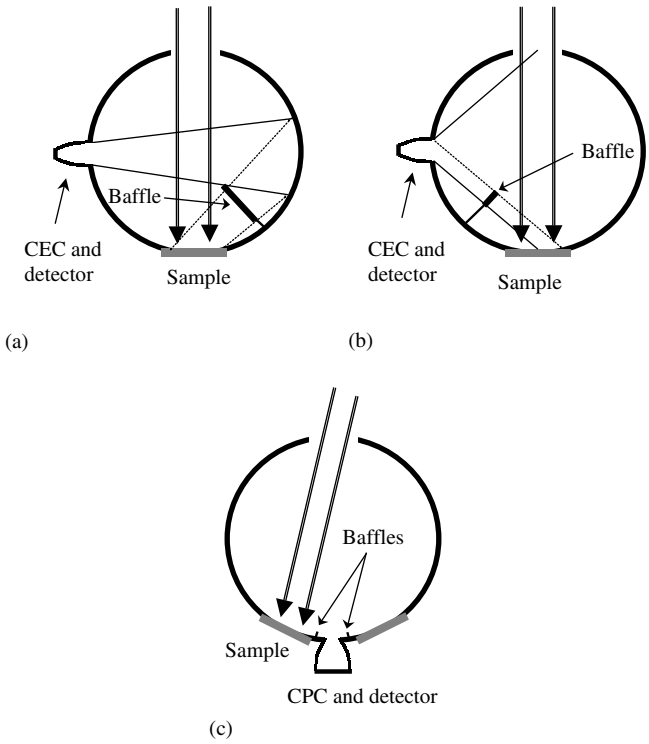

Figure 11. Three isotropic integrating sphere designs.[21] Integrating sphere–detector FOV geometries that minimize measurement errors related to the detector FOV and the sample BRDF. In design (a), both sample and reference reflect no flux directly into the FOV. In design (b), exactly half the flux from both sample and reference is directed into the FOV (assuming that the sample and reference BRDF are symmetric about the plane of incidence). In design (c), (nearly) all of the reflected flux from both sample and reference is directed into the FOV. The compound parabolic and elliptical concentrators (CPC and CEC) are used to sharply delineate the FOV in each design.

6.2 Baffle design

Baffles are frequently required to prevent radiation exchange from one region of the sphere wall to another. For this reason they can be found in most integrating sphere systems, including several absolute methods. For example, for sphere designs that employ a restricted FOV detector, one or two baffles are required to prevent direct radiant interchange between the sample or reference and the region of the sphere wall viewed by the detector. An illustration of the design principle of placing a baffle in an integrating sphere is shown in Figure 12. Fixed dimensions of the sphere, sample, detector FOV, and input beam constrain the baffle positioning to the region abcd in the figure. However, use of baffling is also a trade-off with other induced errors in the sphere behavior. Baffle shading cannot be restricted completely to the intended regions, but occurs to some degree for all areas of the sphere wall. Baffles also have a finite absorption that decreases the throughput for light redirected by the baffles. This is especially true for gold spheres in the IR.[36]

Sphere designers have almost exclusively used baffles with a diffusely reflective coating.[55] However, an alternative design approach is to use high-reflectance specular baffles. Especially in the IR beyond 2.5 μm, the absorptance of specular baffles can be a factor of 5 or 10 lower than for the diffuse alternative. In addition, if they are aligned in a great circle plane of the integrating sphere, then the sphere's property of uniformly distributing radiation over the sphere surface after each reflection tends to

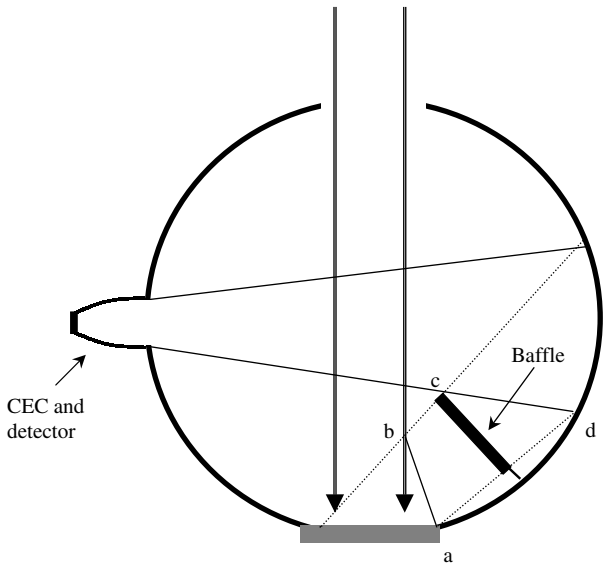

Figure 12. Baffle design geometry and selection. The baffle is placed in a great circle and will be elliptical in shape. To achieve its shading purpose, but not intrude into the input beam nor into the line of sight of the detector, it must be confined to the region abcd. The CEC provides a sharply delineated FOV, which in turn enables a more optimum baffle arrangement.

be preserved. Light from one location that is blocked from reaching a particular point on the sphere is compensated for by light from a symmetrically located position on the opposite side of the baffle. In selecting the position for a specular baffle such as the one shown in Figure 12, one should choose a location that prevents radiation originating at the sample or reference from directly illuminating the detector FOV or detector port. The baffle(s) should also be positioned to avoid sample (reference) reflected light from being redirected to itself or the reference (sample) after a single reflection from the baffle.

6.3 Coating and sample BRDF

It is often assumed that reflections from an integrating sphere's wall are perfectly Lambertian. In practice, this is frequently not the case. In 1987, Gindele and Kohl[56] reported a strong tendency toward specular scattering in a diffuse gold integrating sphere at longer (e.g. 15–20 μm) wavelengths. Oppenheim *et al*.[57] measured the BRDF of five potential diffuse reference standards at 10.6 μm. Sulfur was found to be the most Lambertian; however, flame-sprayed aluminum was preferred for durability reasons. The reflection of the only commercial diffuse gold integrating sphere coating at the time was found to be highly non-Lambertian. Newer commercial diffuse gold surfaces fabricated with a plasma spraying process exhibit[58] a near Lambertian character at 10.6 μm. Hanssen and Kaplan[36] have reported that the latest generation of plasma sprayed integrating sphere coatings have a 10.6 μm BRDF that is very similar to the BRDF of PTFE at 1.5 μm. Smith[59] has developed a similar rough gold coating with nearly Lambertian behavior demonstrated out to 100 μm.

As described in Section 5.2, a technique for reducing the error due to sample scattering characteristics is to characterize the sample BRDF. An approach that is often taken when sample BRDF and integrating sphere throughput uniformity data are not available is to separate the sample reflectance into specular and nonspecular (diffuse) components and perform measurements relative to specular and diffuse standards. This approach can successfully reduce the overall measurement error and uncertainty significantly. However, Roos found it necessary to add a third category of "near-specular" reflected light to the other two to reduce discovered errors further.[60,61] It indicates that the more that is known about the scattering properties of the sample to be characterized, the better.

Analytical and numerical techniques can be used to estimate the impact of a non-Lambertian sphere coating on the measurement of diffuse reflectance values. Habeger[62] used a Fredholm integral equation to estimate the equilibrium distribution of light in an integrating sphere, given a sphere wall coating with a hybrid specular-diffuse character. Hanssen[63] has developed a Monte Carlo ray-tracing routine that allows one to select both an arbitrary BRDF for the sphere wall coating and an arbitrary detector FOV. He found that both the specularity and the wall reflectance value can affect the accuracy of diffuse reflectance measurements. Additional Monte Carlo studies by Prokhorov *et al*.,[64] Crowther[65] and Ohno[66] have evaluated characteristics of sphere performance in other radiometric applications (e.g. characterization of sources) that provide insights useful to the operation and design of spheres for spectrophotometry as well.

6.4 Flat versus curved samples

For the application of integrating sphere theory to calculate the absolute reflectance of samples, the sample shape plays an important role. This is because the sample itself becomes part of the sphere that handles the sample-reflected light. The primary difference between a flat sample and a curved one is that all of the reflected light leaving a flat sample mounted on a sphere wall will be incident on other portions of the sphere and encounter an average sphere wall reflectance that does not include the sample. For a curved sample, on the other hand, some of the sample reflected light can immediately hit other parts of the sample, so that the light will encounter an average sphere wall reflectance

that includes the sample. One result of this effect, for example, is that in spheres with a flat sample and reference, the throughput for sample and reference is different because the sample and reference see each other but not themselves. One approach to counter this effect is to place a baffle between the two. Numerous authors have evaluated these effects, including Taylor,[12] Jacques *et al.*,[24,25] Tardy,[30] and Hisdal.[29]

6.5 Port design

Another critical feature of an integrating sphere is the design of the ports. If one needs to use sphere theory then all of the ports need to be nearly ideal. Then, for empty ports such as the entrance port, light leaving the sphere will not be reflected back into the sphere, e.g. off an external mounting structure. For the sample and reference ports, all the light reflected from the sample and reference will illuminate only the spherical surface of the sphere interior, e.g. not the local walls of a recessed port. For the detector port, its FOV will be determined by the detector and its internal optics and, for example, not additionally limited by the walls of a recessed port design. This means that all ports should have a "knife-edge" design, as illustrated in Figure 13. This is straightforward to achieve in spheres with a thin diffuse coating. For spheres with a volume diffuser coating such as sintered PTFE, for which a finite travel distance (e.g. >6 mm) is required to obtain diffuse scattering a hybrid approach can be used. A tapered "knife-edge" of the sintered PTFE sphere wall can be backed by a substrate coated with $BaSO_4$ near the edge where the PTFE starts to become translucent. In the course of performing integrating sphere angular response uniformity measurements for solar monitoring applications, Milburn and Hollands[67] found response roll-off attributable to the entrance port design. They went on to characterize and analyze the port shape effects in their sphere and demonstrate the advantages of using knife-edge designs.

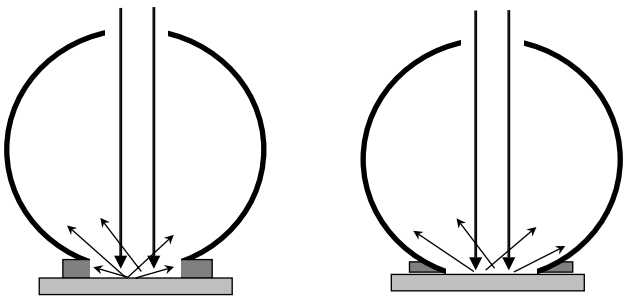

Figure 13. Knife-edge port design. Common integrating sphere port styles featuring (a) a flange mount for convenient sample and component mounting, which recesses the sample from sphere wall and (b) a knife-edge design that minimizes occultation of reflected radiation from sample. Design (a) can result in increased measurement error, while design (b) allows the sphere to directly collect all the sample reflected flux.

The relative sizes of integrating sphere ports are determined by a wide range of factors. These include the instrument's input (to the sphere) beam shape and size, the throughput required for adequate signal-to-noise ratio, sphere wall reflectance, spot size on samples, sample size, reference size, sphere diameter, and level of measurement accuracy. A sphere design must accommodate all of these factors and their interrelationships to be successful. Additional discussion of sources of measurement error and design issues can be found in Clarke and Compton.[68]

7 MODERN SPHERE INSTRUMENTATION FOR SPECTROSCOPY

A large number and variety of integrating spheres have been incorporated into commercial spectrophotometers since the first recording reflectometer was developed by Hardy[69] and manufactured by General Electric in 1933. In their book on reflectance spectroscopy published in 1966, Wendlandt and Hect[70] provide a comprehensive review of contemporary commercial reflectance spectrophotometers. An additional survey of contemporary sphere instruments was conducted by Frei and MacNeil in 1973.[71] Since that time Fourier transform instruments have essentially displaced their dispersive counterparts for IR spectroscopy beyond 2.5 μm and are competing strongly for the near-infrared spectral region as well. Additionally, diffuse gold coatings have extended integrating spheres' spectral range to beyond 20 μm. A large number of sphere spectrophotometer systems, both for the near-infrared and mid-infrared, are commercially available. Integrating sphere accessories are available from many of the spectrophotometer manufacturers as well as from vendors of custom accessories and integrating spheres. We present a partial list of near- and mid-infrared spectrophotometers, for which sphere attachments are compatible, in Table 1. For the purposes of this table, near-infrared is defined as the spectral region between the visible and 2.5 μm (2500 nm).

An example of a near-infrared dispersive double beam spectrophotometer with an integrating sphere attachment is shown in Figure 14. A Perkin–Elmer Lambda 19 UV–vis–NIR monochromator is equipped with an 8-in. diameter integrating sphere designed for both reflectance and transmittance. (The sphere details were designed by Hanssen, the optics and motion mechanism by

(a)

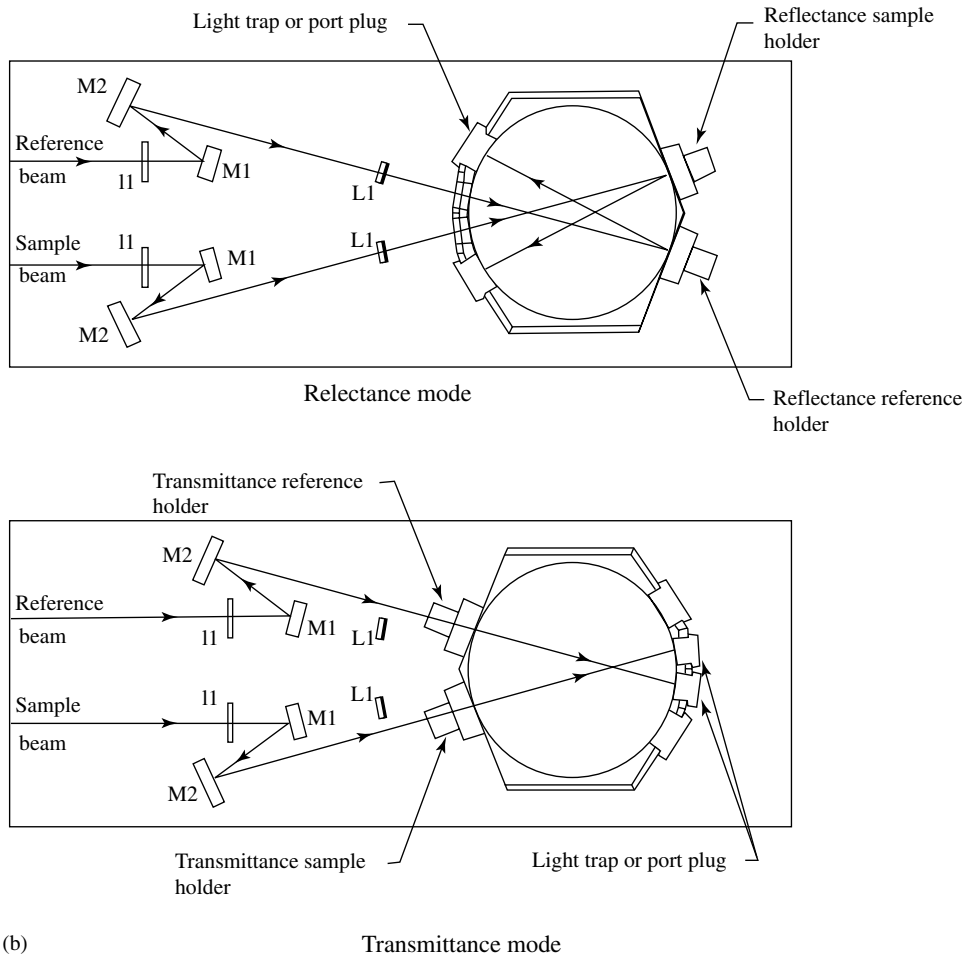

(b)

Figure 14. Photograph (a) and diagrams (b) of the Perkin–Elmer Lambda 19 UV–vis–NIR spectrophotometer with Spectralon™ integrating sphere for reflectance and transmittance. The sphere can be rotated (and the optics (irises, I, mirrors, M, and lenses, L) shifted) to switch the sample and reference ports from a reflectance measurement orientation to one for transmittance measurement. The sample remains mounted on its port for both measurements. Plugs are used for the specular reflectance and entrance ports. (Reproduced by permission of Labsphere.)

Table 1. Manufacturers of spectrophotometers (and spheres) that are compatible with integrating sphere attachments.

Company	WWW site	Instrument type	Waveband[a]
Agilent	chem.agilent.com	DISP	NIR
Analect	orbital-ait.com	DISP, FT-IR	NIR, MIR
Beckman	beckman.com	DISP	NIR
Bio-Rad (Digilab)	bio-rad.com	FT-IR	NIR, MIR
ABB Bomem	bomem.com/	FT-IR	NIR, MIR
Bruker	bruker.com/optics/	FT-IR	NIR, MIR
Hitachi	hii.hitachi.com	DISP	NIR
Labsphere	labsphere.com	Sphere	NIR, MIR
Mattson	mattsonir.com	FT-IR	NIR, MIR
Nicolet	thermonicolet.com	FT-IR	NIR MIR
Perkin–Elmer	instruments.perkinelmer.com	DISP, FT-IR	NIR, MIR
Shimadzu	ssi.shimadzu.com	DISP, FT-IR	NIR, MIR
Varian	varianinc.com	DISP	NIR

[a]NIR, near-infrared; MIR, mid-infrared.

Kevin Carr of Labsphere, and the accessory manufactured and commercialized by Labsphere.) Features of this design include symmetrical arrangement of sample and reference beam paths, knife-edge sample and reference ports, end-on photomultiplier tube detector with improved spatial and angular response, crossed beam paths to enable 6° incidence on sample and reference, and rotation of the sphere to switch samples from reflectance to transmittance geometry.

An example of a mid-infrared FT-IR spectrophotometer with an integrating sphere attachment is shown in Figure 15. A Bomem MB-100 FT-IR is equipped with a diffuse gold integrating sphere accessory mounted on the top of the FT-IR where access to the beam is available. A purge enclosure (not shown) covers the accessory during measurement. The sample is mounted on a holder in the sphere center that is attached to a removable cover seen on top of the sphere in Figure 15. Via rotation of the sample mount cover, the angle of incidence can be varied. The beam is brought via a focusing mirror on the left side of the accessory through an entrance port on the left of the sphere to the sample. A pair of removable port plugs enables the measurement of the diffuse components of reflection for 10° and 60° incidence. A reference measurement can be made either with (1) a reference sample that is mounted back-to-back with the sample (and a 180° rotation), or (2) the back sphere wall, by a 90° rotation of an off-center-mounted sample to move it out of the input beam.

Figure 15. Photograph of Bomem MB-100 w/gold sphere. The gold integrating sphere is mounted in the standard sample compartment area above the FT-IR. The sphere's entrance port can be seen on its left side facing the focusing mirror. The larger port cover next to it can be removed for separation of diffuse and specular (reflectance) components. The sample is loaded and rotated from the top of the sphere and located at its center. An ellipsoidal mirror (out of view) is used to focus the small exit port underneath the sphere onto the detector (white dewar at the right) detector. The reference measurement is made, after rotation of the sample, with a reference standard mounted back-to-back with the sample. (Reproduced by permission of ABB Bomem Inc.)

An example of an IR sphere that has been adapted to several FT-IR spectrophotometers is shown in Figure 16. It is the RSA-FT-IR-I diffuse gold sphere accessory manufactured by Labsphere. This particular sphere is designed for convenience and versatility. While perhaps sacrificing some degree of measurement accuracy as compared with larger spheres, the measurement of hemispherical reflectance has a significant advantage over the reflectance quantity measured with large solid-angle biconical devices. The small size (10 cm (4 in.) diameter) allows it to fit in many FT-IR sample compartments. The input beam is switched between sample and reference via a mirror mounted in the sphere center. Both transmittance (in substitution mode)

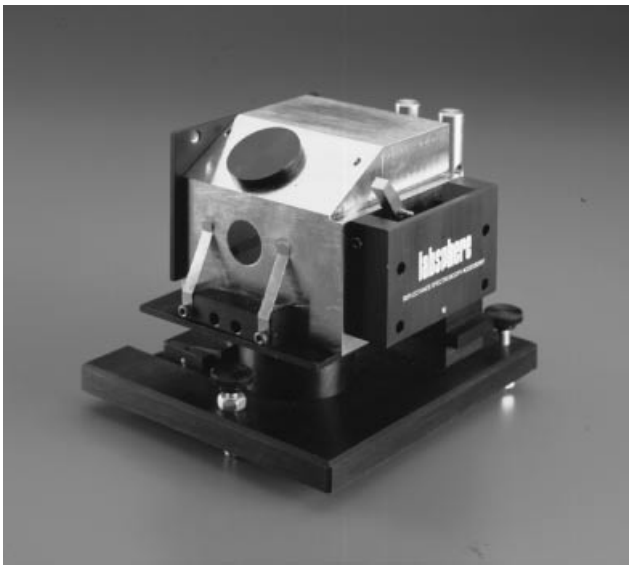

(a)

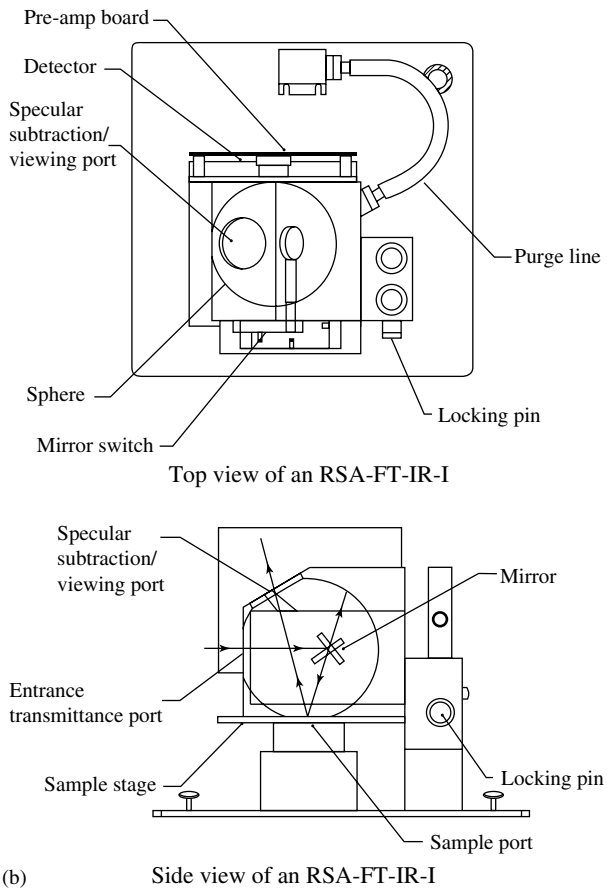

(b)

Figure 16. Photograph (a) and diagrams (b) of Labsphere generic gold sphere for FT-IR spectrophotometers. The compact 4-in. diameter sphere design allows easy adaptation to most sample compartments. Switching between sample and reference measurements is achieved by flipping a small mirror located inside the integrating sphere. Samples can be clamped to the front for transmittance or mounted from underneath for reflectance. (Reproduced by permission of Labsphere Inc.)

and reflectance can be measured for samples mounted on the side and bottom of the sphere, respectively. A specular subtraction port enables a diffuse component measurement.

The integrating sphere accessories shown here are intended as a set of examples and represent only a small portion of the many that are commercially available from a variety of accessory and spectrophotometer manufacturers.

8 SUMMARY AND DISCUSSION

The use of integrating spheres for optical property characterization of materials has a long history extending back to the early 1900s. Despite the development of other methods for evaluating diffusely scattering materials, for most users, integrating sphere devices remain preferable for obtaining more accurate results. Nevertheless, a wide array of potential sources of error can be encountered when working with integrating spheres and their associated methods. Much of the problem lies in the inherent difficulty and challenge of uniformly measuring all of the scattered light from a sample independent of scattering profile. The problems and the size of the associated errors are significantly larger in the mid-infrared than in the near-infrared. This is manifested in numerous ways, from discrepancies in round-robin measurements,[51] to the order of magnitude larger uncertainties on available standard artefacts available from NMIs for the mid-infrared as compared with the near-infrared.

Recent developments in materials development as well as computer modeling of integrating sphere systems should result in lower uncertainties for standard artefacts, as well as spheres with improved performance, thus leading to more accurate optical property measurements and data. As computer processor power continues to increase, computer simulation models of integrating sphere behavior should become more sophisticated, precise and accurate. Studies using better computer modeling tools should lead to consistently optimized sphere designs. New design concepts will be able to be thoroughly evaluated without the cost and effort of constructing the actual device and performing extensive laboratory tests. Among other potential improvement benefits, greater sphere throughput (efficiency) could expand the use of integrating spheres relative to devices that have a throughput advantage (but are less accurate) such as biconical mirror systems.

DISCLAIMER

Certain commercial equipment, instruments, and materials are identified in this paper to foster understanding. Such identification does not imply recommendation or endorsement by the NIST.

ABBREVIATIONS AND ACRONYMS

BRDF	Bidirectional Reflectance Distribution Function
CEC	Compound Elliptical Concentrator
CIE	International Commission on Illumination
CPC	Compound Parabolic Concentrator
FOV	Field of View
NIST	National Institute of Standards and Technology
NMIs	National Measurement Institutes
NPL	National Physical Laboratory
NRC	National Research Council
PTB	Physikalische Technische Bundesanstalt
PTFE	Poly(tetrafluoroethylene)
UV–vis–NIR	Ultraviolet–Visible–Near-infrared

REFERENCES

1. W. Budde, *J. Res. Natl. Bur. Stnd. (US)*, **80A**, 585 (1976).
2. CIE, 'Absolute Methods for Reflection Measurement', CIE Technical Report, CIE Publ. No. 44, Vienna (1990).
3. CIE, 'International Lighting Vocabulary', CIE Publ. No. 17.4, Geneva (1987).
4. W.E. Sumpner, *Phil. Mag. J. Sci.*, **35**, 81 (1893).
5. V.R. Ulbricht, *Elektrotech. Zeit.*, **29**, 595 (1900).
6. E.B. Rosa and A.H. Taylor, *Trans. Illum. Eng. Soc.*, **11**, 453 (1916).
7. A.H. Taylor, *J. Opt. Soc. Am.*, **4**, 9 (1920).
8. F.A. Benford, *G.E. Rev.*, **23**, 72 (1920).
9. C.H. Sharp and W.F. Little, *Trans. Illum. Eng. Soc.*, **15**, 802 (1920).
10. E. Karrer, *Bur. Std. Sci. Papers*, **17**, 203 (1921).
11. F. Benford, *J. Opt. Soc. Am.*, **24**, 165 (1934).
12. A.H. Taylor, *J. Opt. Soc. Am.*, **25**, 51 (1935).
13. A.C. Hardy, *J. Opt. Soc. Am.*, **28**, 360 (1938).
14. J.L. Michaelson, *J. Opt. Soc. Am.*, **28**, 365 (1938).
15. W. Budde, *J. Opt. Soc. Am.*, **50**, 217 (1960).
16. K.A. Snail and L.M. Hanssen, 'Reflectance Measurements of Diffusing Surfaces Using Conic Mirror Reflectometers', in "Applied Spectroscopy: a Compact Reference for Practitioners", eds J. Workman and A. Springsteen, Academic Press, New York, 269–275 (1998).
17. R.R. Willey, *Appl. Spectrosc*, **30**, 593 (1976).
18. F.J.J. Clarke, 'Photometric Standards for Mid-infrared Spectrometry', in "Handbook of Vibrational Spectroscopy", eds J.M. Chalmers and P.R. Griffiths, John Wiley & Sons, London 891–898 Vol. 1 (2002).
19. H.L. Tardy, *Appl. Opt.*, **24**, 3914 (1985).
20. W.W. Welford and R. Winston, 'High Collection Nonimaging Optics', Academic Press, New York (1989).
21. K.A. Snail and L.M. Hanssen, *Appl. Opt.*, **28**, 1793 (1989).
22. K.A. Snail and K.F. Carr, *Proc. Soc. Photo.-Opt. Instrum. Eng.*, **643**, 75 (1986).
23. E. Karrer, *Sci. Pap. Bur. Stand.*, No. 415 (1921).
24. J.A. Jacques, W. McKeehan, J. Huss, J.M. Dimitroff and H.F. Kuppenheim, *J. Opt. Soc. Am.*, **45**, 781 (1955).
25. J.A. Jacques and H.F. Kuppenheim, *J. Opt. Soc. Am.*, **45**, 460 (1955).
26. H.L. Tardy, *J. Opt. Soc. Amer. A*, **5**, 241 (1988).
27. D.G. Goebel, *Appl. Opt.*, **6**, 125 (1967).
28. L.M. Hanssen, *Appl. Opt.*, **28**, 2097 (1989).
29. B.J. Hisdal, *J. Opt. Soc. Am.*, **55**, 1122 (1965).
30. H.L. Tardy, *J. Opt. Soc. Am. A*, **8**, 1411 (1991).
31. J.E. Clare, *J. Opt. Soc. Am. A*, **15**, 3086 (1998).
32. H. Korte and M. Schmidt, *Lichttechnik*, **19**, 135A (1967).
33. D.K. Edwards, J.T. Gier, K.E. Nelson and R.D. Roddick, *Appl. Opt.*, **51**, 1279 (1961).
34. J.A. Van den Akker, L.R. Dearth and W.M. Shillcox, *J. Opt. Soc. Am.*, **56**, 250 (1966).
35. L.M. Hanssen, 'Integrating Sphere for Absolute Infrared Diffuse Reflectance Measurement', presented at the 1996 CORM Annual Meeting, Gaithersburg, MD (1996).
36. L.M. Hanssen and S.G. Kaplan, *Anal. Chim. Acta*, **380**, 289 (1998).
37. J.S. Preston, *Trans. Opt. Soc. London*, **31**, 15 (1929).
38. W.E. Middleton and C.L. Sanders, *J. Opt. Soc. Am.*, **41**, 419 (1951).
39. W. Budde, *Die Farbe*, **7**, 17 (1958).
40. O.E. Miller and A.J. Sant, *J. Opt. Soc. Am.*, **48**, 828 (1958).
41. L.M. Hanssen, *Appl. Opt.*, **28**, 2097 (1989).
42. V.A. Reule, *Zeiss Mitt.*, **2**, no. 9, 371–387 (1962). A. Reule, *Optik*, **49**, 499–504 (1978).
43. D. Sheffer, U.P. Oppenheim and A.D. Devir, *Appl. Opt.*, **30**, 3181 (1991).
44. D. Sheffer, U.P. Oppenheim and A.D. Devir, *Appl. Opt.*, **29**, 129 (1990).
45. W. Budde and C.X. Dodd, *Die Farbe*, **19**, 94 (1970).
46. W.H. Venable, J.J. Hsia and V.R. Weidner, *J. Res. Natl. Bur. Stnd. (US)*, **82**, 29 (1977).
47. C.P. Tingwaldt, *Optik*, **9**, 323 (1952).
48. A.S. Toporets, *Opt. Spectrosc.*, **7**, 471 (1959).
49. W. Erb, *Lichttechnik*, **25**, 345 (1973).
50. W. Erb, *PTB Mitteilungen*, **87**, 283 (1977).
51. R.R. Willey, *Proc. Soc. Photo.-Opt. Instrum. Eng.*, **807**, 140 (1987).
52. L.M. Hanssen, *Appl. Opt.*, **40**, 3196 (2001).
53. A.C. Hardy and O.W. Pineo, *J. Opt. Soc. Am.*, **21**, 502 (1931).
54. W.T. Welford and R. Winston, 'High Collection Nonimaging Optics', Academic Press, New York (1989).
55. A.C.M. de Visser and M. van der Woude, *Lighting Res. Technol.*, **12**, 42 (1980).

56. K. Gindele and M. Köhl, *Sol. Energy Mates.*, **16**, 167 (1987).
57. U.P. Oppenheim, M.G. Turner and W.L. Wolfe, *Infrared Phys. Technol.*, **35**, 873 (1994).
58. L.M. Hanssen, 'New Instrument Development at the National Institute of Standards and Technology for Spectral Diffuse Reflectance and Transmittance Measurement', in "Spectrophotometry, Luminescence and Colour; Science and Compliance", eds C. Burgess and D.G. Jones, Elsevier, New York, 115–128 (1995).
59. S.M. Smith, *Proc. Soc. Photo.-Opt. Instrum. Eng.*, **1753**, 47 (1992).
60. K. Grandin and A. Roos, *Appl. Opt.*, **33**, 6098 (1994).
61. D. Ronnow and A. Roos, *Rev. Sci. Instrum.*, **66**, 2411 (1995).
62. C.C. Habeger, *J. Opt. Soc. Am. A*, **11**, 2130 (1994).
63. L.M. Hanssen, *Appl. Opt.*, **35**, 3597 (1996).
64. A.V. Pokhorov, V.I. Sapritsky and S.N. Mekhontsev, *Proc. Soc. Photo.-Opt. Instrum. Eng.*, **2815**, 118 (1996).
65. B.G. Crowther, *Appl. Opt.*, **35**, 5880 (1996).
66. Y. Ohno, *Appl. Opt.*, **33**, 2637 (1994).
67. D.I. Milburn and K.G.T. Hollands, *Opt. Commun.*, **115**, 158 (1995).
68. F.J.J. Clarke and J.A. Compton, *Color Res. Appl.*, **11**, 253 (1986).
69. A.C. Hardy, *J. Opt. Soc. Am.*, **28**, 360 (1938).
70. W.W. Wendlandt and H.G. Hecht, 'Reflectance Spectroscopy', Interscience Publishers, New York (1966).
71. R.W. Frei and J.D. MacNeil, 'Diffuse Reflectance in Environmental Problem-solving', CRC Press, Cleveland (1973).

1 APPENDIX

Details of the absolute reflectance method developed by Hanssen are provided here. A sphere measurement geometry for which the method has been applied is shown in Figure 9 and described in Section 5.1. Additional sample BRDF and integrating sphere throughput mapping measurement results are performed and used in the method. The directional-hemispherical reflectance value is obtained by combining four measured quantities: (1) a ratio of sample (V_s) to reference (V_r) measurements with the sphere system, V_s/V_r; (2) a ratio of sample-removed (V_{0s}) to reference (V_{0r}) measurements with the sphere system, V_{0s}/V_{0r}; (3) the relative sphere throughput, as a function of polar (θ) and azimuthal (ϕ) angles (relative to the sample surface), $\tau_s(\theta,\phi)/\tau_{s0}$, where τ_{s0} is the throughput for the direction corresponding to the sample-removed measurement (generally, the specular direction); and (4) the relative BRDF of the sample for the incidence (γ) angle of the sphere measurement, $f(\gamma;\theta,\phi)/f_0$, where f_0 is an arbitrary constant.

The sample and reference single beam measurements can be expressed as

$$V_s = \tau_{avg} \cdot \rho_{\gamma,h} \cdot k \cdot \Phi_0 \tag{13}$$

$$V_r = \tau_{r0} \cdot k \cdot \Phi_0 \tag{14}$$

$$V_{0s} = \tau_{0s} \cdot k \cdot \Phi_0 \tag{15}$$

and

$$V_{0r} = \tau_{0r} \cdot k \cdot \Phi_0 \tag{16}$$

where k is the instrument function, Φ_0 is the incident flux, and

$$\tau_{avg} = \frac{1}{\rho_{\gamma,h}} \times \int_0^{2\pi}\int_0^{\frac{\pi}{2}} f(\gamma;\theta,\phi)\cdot\cos(\theta)\cdot\tau_s(\theta,\phi)\cdot\sin(\theta)\cdot d\theta\cdot d\phi \tag{17}$$

is the average sphere throughput for the flux distribution reflecting off the sample. For a Lambertian diffuser,

$$\tau_{avg} = \frac{1}{2\pi}\int_0^{2\pi}\int_0^{\frac{\pi}{2}} \tau_s(\theta,\phi)\cdot\sin(\theta)\cdot d\theta\cdot d\phi \tag{18}$$

If in addition, the throughput is uniform, i.e. $\tau_s(\theta,\phi) = \tau_{s0}$, (except for $\tau_s(\theta,\phi) = 0$, for $(\theta,\phi \in$ sphere ports, i) then

$$\tau_{avg} = \tau_{s0}\left(1 - \sum_i f_i\right) \tag{19}$$

where the summation is made over the empty ports of the sphere, f_i is the exchange factor between the ith port and sphere wall, which equals A_i/A_{sp}, the ratio of the ith port area to the sphere area. The directional-hemispherical reflectance can also be obtained through integration of the BRDF of the sample over the hemisphere:

$$\rho_{\gamma,h} = \int_0^{2\pi}\int_0^{\frac{\pi}{2}} f(\gamma;\theta,\phi)\cdot\cos(\theta)\cdot\sin(\theta)\cdot d\theta\cdot d\phi \tag{20}$$

The ratios of sample and reference measurements, V_s/V_r and sample-removed and reference measurements V_{0s}/V_{0r} are obtained by ratioing equations (13) and (14), and equations (15) and (16), resulting in

$$\frac{V_s}{V_r} = \frac{\tau_{avg}}{\tau_{r0}} \cdot \rho_{\gamma,h} \tag{21}$$

and

$$\frac{V_{0s}}{V_{0r}} = \frac{\tau_{0s}}{\tau_{0r}} = \frac{\tau_{s0}}{\tau_{r0}} \tag{22}$$

The difference between τ_{x0} and τ_{0x} is due to the change in the sample contribution to the average sphere wall reflectance from equation (2). The difference is proportional and drops out of the ratios in equation (22). If we

solve equation (21) for $\rho_{\gamma,\mathrm{h}}$, and substitute for $\tau_{\mathrm{r}0}$ from equation (22), we obtain

$$\rho_{\gamma,\eta} = \frac{V_{\mathrm{s}}}{V_{\mathrm{r}}}\frac{V_{\mathrm{r}0}}{V_{\mathrm{s}0}}\frac{\tau_{\mathrm{s}0}}{\tau_{\mathrm{avg}}} \tag{23}$$

We substitute $\rho_{\gamma,\mathrm{h}}$ from equation (20) into equation (17), and finally substitute the result τ_{avg} into equation (23). We obtain the following formula for the reflectance:

$$\rho_{\gamma,\mathrm{h}} = \frac{V_{\mathrm{s}}}{V_{\mathrm{r}}}\frac{V_{0\mathrm{r}}}{V_{0\mathrm{s}}} \times \left[\frac{\displaystyle\int_0^{2\pi}\int_0^{\frac{\pi}{2}} f(\gamma;\theta,\phi)/f_0 \cdot \sin(2\theta)\cdot \mathrm{d}\theta \cdot \mathrm{d}\phi}{\displaystyle\int_0^{2\pi}\int_0^{\frac{\pi}{2}} f(\gamma;\theta,\phi)/f_0 \cdot \tau_{\mathrm{s}}(\theta,\phi)/\tau_{\mathrm{s}0} \cdot \sin(2\theta)\cdot \mathrm{d}\theta \cdot \mathrm{d}\phi}\right] \tag{11}$$

Equation (11) puts the absolute directional-hemispherical reflectance $\rho_{\gamma,\mathrm{h}}$ in terms of the four measured quantities: the direct sample and reference measurements ratio, a second measurement ratio with sample-removed, the relative throughput, and the relative BRDF.

One way of looking at the measurements of $V_{\mathrm{r}0}$ and $V_{0\mathrm{r}}$ is that they are used to account for drift between measurements as well as the change in overall sphere throughput that occurs with the removal of the sample for the measurement of $V_{\mathrm{s}0}$. Effectively, the four measurements that form the term outside the brackets of the right-hand side of equation (11) reduce to a ratio of the sample-in signal to the sample-out signal (properly corrected for sphere throughput change). This means that the particular arrangement of the V_{r}'s is not critical since their absolute level ratios out. Because of higher-order effects, it is nevertheless preferable to use a highly symmetric arrangement as in Figure 9. Measurements of $V_{0\mathrm{s}}/V_{0\mathrm{r}}$ in Hanssen[52] for an IR sphere with this geometry vary from 1 by only 0.2% to 0.5%. In this case the sample-removed measurement becomes unnecessary for diffuse samples where the other sources of uncertainty may be significantly larger. For specular samples, the sample-removed measurement is useful to obtain the highest accuracy.

By combining BRDF and integrating sphere measurements, this method appears to combine redundant information, since a complete BRDF measurement over a hemisphere of output angles can also be used to obtain $\rho_{\gamma,\mathrm{h}}$. However, it is difficult to obtain sufficiently accurate BRDF over a sufficiently large fraction of the hemisphere (to viewing angles near grazing) to obtain an accurate $\rho_{\gamma,\mathrm{h}}$ value. For the method described above, however, only relative BRDF are required. Since equation (11) contains a ratio of integrals over the same hemispherical angular range, if the measured data are not complete or require extrapolation, the ratio effectively removes a significant part of the error that would remain in both individual components.